HIERARCHICAL MULTISCALE MODELING OF TIRE-SOIL INTERACTION FOR OFF-ROAD MOBILITY SIMULATION

Hiroki Yamashita
Guanchu Chen

Department of Mechanical Engineering
The University of Iowa
4225 Seamans Center
Iowa City, IA 52242

Yeefeng Ruan
Paramsothy Jayakumar

U.S. Army TARDEC
Warren, MI 48397

*Hiroyuki Sugiyama**

Department of Mechanical Engineering
The University of Iowa
2139 Seamans Center
Iowa City, IA 52242
**hiroyuki-sugiyama@uiowa.edu*

ABSTRACT

A high-fidelity computational terrain dynamics model plays a crucial role in accurate vehicle mobility performance prediction under various maneuvering scenarios on deformable terrain. Although many computational models have been proposed using either finite element (FE) or discrete element (DE) approaches, phenomenological constitutive assumptions in FE soil models make the modeling of complex granular terrain behavior very difficult and DE soil models are computationally expensive, especially when considering a wide range of terrain. To address the limitations of exiting deformable terrain models, this paper presents a hierarchical FE-DE multiscale tire-soil interaction simulation capability that can be integrated in the monolithic multibody dynamics solver for high-fidelity off-road mobility simulation using high-performance computing techniques. It is demonstrated that computational cost is substantially lowered by the multiscale soil model as compared to the corresponding pure DE model while maintaining the same accuracy. The multiscale tire-soil interaction model is validated against the soil bin mobility test data under various wheel load and tire inflation pressure conditions, thereby demonstrating the potential of the proposed method for resolving challenging vehicle-terrain interaction problems.

Keywords: Tire-soil interaction, off-road mobility simulation. multibody dynamics, multiscale methods, finite element methods, discrete element methods.

1. INTRODUCTION

A high-fidelity computational terrain dynamics model is essential for physics-based off-road mobility simulations in achieving accurate mobility performance prediction under various vehicle maneuvering scenarios on deformable terrain [1]. Granular terrain dynamics is complex, involving highly nonlinear anisotropy of strength and strain localization. Most computational soil models currently in use utilize either the finite element (FE) approach [2-6] or the discrete element (DE) approach [7-12]. In the FE model, soil is approximated as a continuum and its failure behavior including soil hardening characteristics is described by phenomenological constitutive equations such as the Mohr-Coulomb and the capped Drucker-Prager failure criteria [2]. While cohesive soil behavior is well predicted using continuum FE models, use of phenomenological constitutive assumptions makes accurate modeling of complex granular material behavior and its parameter identification very difficult.

DE models, therefore, have gained acceptance in modeling the grain-scale granular material behavior. Since the material behavior is modeled by discrete particles with frictional contact, complex granular soil behavior including history-dependent strain localization can be predicted in a relatively straightforward manner. Thus, DE approach has been widely utilized for the analysis of various geotechnical applications [8]. Critical challenges still lie in high computational intensity in application to off-road mobility simulation since a wide range of terrain needs to be modeled in vehicle maneuvering simulations, resulting in large-dimensional DE models. Various attempts, therefore, have been pursued from the computational and modeling perspectives, including use of high-performance computing (HPC) capabilities with Graphic Processor Unit (GPU) [13,14] and complementarity rigid contact approach in place of the compliant contact approach [15], etc.

In order to exploit advantages of both the FE and DE soil models, a coupled FE-DE soil model is proposed for tire-soil interaction simulations [16]. In this model, the DE model is used to describe the surface layers of terrain to model the dynamic interaction between soil and a rolling tire, while the FE model is utilized to describe the subsurface layers to reduce the overall model dimensionality. The coupled FE and DE simulation is also referred as *concurrent* multiscale simulation in the field of computational geomechanics, in which DE models are introduced to a macroscale continuum FE soil model to predict the localized grain-scale granular material behavior with contact and impact [17,18]. To couple the FE and DE models in the interface region, either kinematic constraint or contact condition needs to be imposed, and special care needs to be exercised to ensure that mechanical properties of the DE and FE soil models are consistent in the interface region. In contrast, the *hierarchical* multiscale method for geomaterials utilizes the FE model to predict macroscale deformation of geomaterials as a continuum, while the phenomenological constitutive relation, such as the capped Drucker-Prager failure model, is replaced by the physical response of grain-scale DE model defined using the representative volume element (RVE) [19-22]. In other words, the stress response at the FE quadrature point is obtained directly from the DE model without resorting to the phenomenological constitutive model. The DE particles do not occupy the entire model space, but only multiple RVEs are defined at FE quadrature points. Thus, the DE model size can be substantially decreased as compared to the pure DE models [21,22]. Furthermore, boundary conditions for granular materials can be imposed in a straightforward manner using FE meshes.

Despite the unique features and the potential of the hierarchical FE-DE multiscale approach for modeling complex soil behavior which the use of assumed phenomenological constitutive models can result in inaccurate prediction, the hierarchical multiscale modeling for vehicle-terrain interaction has not been addressed due to the complexity in integrating the FE and DE models in general multibody dynamics computer algorithm required for physics-based off-road vehicle mobility simulations. It is, therefore, the objective of this study to develop a hierarchical multiscale tire-soil interaction simulation capability that can be integrated in the monolithic multibody dynamics solver for high-fidelity off-road mobility simulation using high-performance computing techniques. For this purpose, the FE-based flexible multibody dynamics tire-soil interaction simulation solver developed in the authors' previous study [6] is generalized for a hierarchical multiscale terrain dynamics model as shown in Fig. 1 in this study. In particular, a scale-bridging algorithm between the upper-scale FE terrain model in the multibody dynamics solver and lower-scale RVE models in the DE solve is developed to establish new multiscale off-road mobility simulation capability, considering multibody vehicle components with nonlinear FE tires. Furthermore, to enable parallelized DE simulations for multiple RVEs, a distributed-memory parallel computing algorithm is developed for the lower-scale models using Message Passing Interface (MPI), while the share-memory parallel computing is used for solving the multibody dynamics equations with the upper-scale soil models with OpenMP. Accuracy and computational efficiency of the multiscale terrain dynamics models are assessed by comparison with the pure DE model as well as the test data for the triaxial soil compression test and the soil bin mobility test scenarios. The moving soil patch algorithm [6,11] is also generalized to the multiscale terrain dynamics model such that the multiscale soil model is considered only in the vicinity of the rolling tire to reduce the overall model dimensionality for off-road mobility simulation.

2. HIERARCHICAL FE-DE MULTISCALE MODELING

2.1 Upper-Scale Finite-Element Model

The upper-scale continuum model is developed using the nonlinear finite element method. A brick element integrated in the monolithic multibody dynamics solver is generalized to account for the grain-scale granular material behavior using the lower-scale DE model at the quadrature points within the element. The global position vector of an arbitrary point in the element is defined by

$$\mathbf{r} = \mathbf{N}(\xi, \eta, \zeta)\mathbf{e} \tag{1}$$

where $\mathbf{N}$ is the shape function matrix and $\mathbf{e}$ is the nodal coordinate vector. ξ, η, ζ are the element natural coordinates. The Green-Lagrange strain tensor is given by [23]

$$\mathbf{E} = \frac{1}{2}(\mathbf{F}^T\mathbf{F} - \mathbf{I}) \tag{2}$$

where $\mathbf{F}$ is the global position vector gradient tensor defined by

$$\mathbf{F} = \frac{\partial \mathbf{r}}{\partial \mathbf{X}} = \bar{\mathbf{J}}(\mathbf{J})^{-1} \tag{3}$$

and $\bar{\mathbf{J}} = \partial \mathbf{r}/\partial \mathbf{x}$ and $\mathbf{J} = \partial \mathbf{X}/\partial \mathbf{x}$. The vector $\mathbf{X}$ defines the global position vector at an arbitrary reference configuration. The generalized internal force $\mathbf{Q}_s$ can then be obtained as

$$\mathbf{Q}_s = \int_{V_0} \left(\frac{\partial \boldsymbol{E}}{\partial \mathbf{e}}\right)^T \boldsymbol{S}\, dV_0 \tag{4}$$

where $\boldsymbol{E}$ is a vector of the Green-Lagrange strain tensor obtained from Eq. 2, while $\boldsymbol{S}$ is a vector of the second Piola–Kirchhoff (PK) stresses and dV_0 is the infinitesimal volume at the reference configuration. Using the principle of virtual work in dynamics, the equations of motion of the element can be obtained as [6]

$$\mathbf{M}\ddot{\mathbf{e}} = \mathbf{Q}_s + \mathbf{Q}_e \tag{5}$$

where $\mathbf{M}$ is the constant generalized mass matrix and $\mathbf{Q}_e$ is the generalized external force vector that can include the contact forces with the rolling tire.

2.2 Lower-Scale Discrete-Element Model

To define the stress response at a quadrature point within the element, the representative volume element (RVE) is defined using the DE approach as shown in Fig. 1. The RVE is subjected to spatial periodic boundaries to predict homogenized stress responses of granular material at the material point within the element. In the DE simulation, the Hertzian compliant normal contact force model is used as [8]

$$F_n = \frac{2E}{3(1-\nu^2)}\sqrt{r_e \delta_n} \cdot \delta_n \tag{6}$$

where E, ν, r_e, and δ_n are, respectively, Young's modulus, Poisson's ratio, equivalent particle radius, and assumed penetration between two particles in contact. A Mindlin-type tangential force model is used to define the state of sticking, while the Coulomb friction model is used in the sliding state as [8]

$$F_t = \begin{cases} \dfrac{4G}{2-\nu}\sqrt{r_e \delta_n} \cdot \delta_t & \cdots \quad \text{sticking} \\ \mu F_n & \cdots \quad \text{sliding} \end{cases} \tag{7}$$

where μ and δ_t are, respectively, the friction coefficient and tangential deformation between two particles in contact. The rolling resistance moment is also considered to describe moments exerted on non-spherical particles in contact as [24]

$$M_r = \begin{cases} \beta K_n r_e^2 \eta^2 \cdot \theta_r & \cdots \quad \text{sticking} \\ \eta F_n r_e & \cdots \quad \text{sliding} \end{cases} \tag{8}$$

where β and η are rolling resistance parameters, while θ_r is torsional deflection between two particles.

To obtain the history-dependent stress response using the RVE, incremental strain tensor $\Delta\boldsymbol{\varepsilon}$ at the quadrature point in the finite element is calculated at each time step and is used to deform the corresponding RVE by changing the coordinates of the RVE planes [8]. For this, the logarithmic strains (i.e., true strains) in reference to the current configuration is evaluated as

$$\boldsymbol{\varepsilon} = \sum_{i=1}^{3} \ln(\lambda_i)\mathbf{n}_i \otimes \mathbf{n}_i \tag{9}$$

where λ_i is the i-th eigenvalue of spatial stretch tensor $\mathbf{V}$ given from the polar decomposition of the displacement gradient tensor $\mathbf{F} = \mathbf{VR}$ with the rotation tensor $\mathbf{R}$. The vector $\mathbf{n}_i$ is the associated eigenvector. Having completed the DE simulation under the prescribed strain boundary condition at each time step of the upper-scale model, the RVE particle data at the deformed configuration is saved for use in the next time step and the homogenized Cauchy stress tensor of the deformed RVE can then be calculated as [8]

$$\boldsymbol{\sigma} = \frac{1}{V}\sum_{N_c} \mathbf{d}^c \otimes \mathbf{f}^c \tag{10}$$

where $\mathbf{f}^c$ is the inter-particle contact force vector, while $\mathbf{d}^c$ is the relative displacement vector of particles in contact. V is the volume of the deformed RVE and N_c is the total number of contact in the RVE. Furthermore, the homogenized tangent moduli tensor can be obtained as [21]

$$\frac{\partial\boldsymbol{\sigma}}{\partial\boldsymbol{\varepsilon}} = \frac{1}{V}\sum_{N_c}(k_n\mathbf{n}^c \otimes \mathbf{d}^c \otimes \mathbf{n}^c \otimes \mathbf{d}^c + k_t\mathbf{t}^c \otimes \mathbf{d}^c \otimes \mathbf{t}^c \otimes \mathbf{d}^c) \tag{11}$$

where $\mathbf{n}^c$ and $\mathbf{t}^c$ are unit normal and tangent vectors of contact plane between two particles in contact. To obtain the generalized internal force vector of the FE model in Eq. 4, the homogenized Cauchy stress tensor is converted to the second PK stress tensor as [23]:

$$\mathbf{S} = J\,\mathbf{F}^{-1}\,\boldsymbol{\sigma}\,\mathbf{F}^{-T} \tag{12}$$

where $J = \det|\mathbf{F}|$. The preceding equation is used to define the internal forces of the upper-scale FE model in Eq. 4. Accordingly, history-dependent stress responses of granular materials, predicted by the DE models, can be incorporated in the FE model and the conventional phenomenological constitutive assumption can be eliminated [19-22].

3. HIERARCHICAL MULTISCALE TIRE-SOIL INTERACTION MODEL

3.1 Integration of the Multiscale Terrain Model in Monolithic Off-Road Mobility Solver

The heretical multiscale soil model is incorporated into the flexible multibody dynamics solver for off-road mobility simulation, involving interconnected vehicle components and nonlinear FE tire models. While the DE solvers are involved in the stress calculation at quadrature points within elements, the dynamic response of the multiscale soil model is defined by the upper-scale FE model. Thus, the flexible multibody dynamics computational algorithm developed for the FE-based deformable tire-soil interaction simulation [6] can be utilized as the basis for incorporating the multiscale soil model. The following governing equations for the upper-scale models can be obtained and integrated forward in time at each time step:

$$\left.\begin{array}{ll}
\mathbf{M}_r\ddot{\mathbf{q}}_r + \mathbf{C}_{\mathbf{q}_r}^T\boldsymbol{\lambda} = \mathbf{Q}_r(\mathbf{q}_r, \mathbf{e}_t, \dot{\mathbf{q}}_r, \dot{\mathbf{e}}_t) & \cdots\ \text{Rigid vehicle components} \\
\mathbf{M}_t\ddot{\mathbf{e}}_t + \mathbf{C}_{\mathbf{e}_t}^T\boldsymbol{\lambda} = \mathbf{Q}_t(\mathbf{q}_r, \mathbf{e}_t, \mathbf{e}_s, \dot{\mathbf{q}}_r, \dot{\mathbf{e}}_t, \dot{\mathbf{e}}_s, \boldsymbol{\alpha}) & \cdots\ \text{Nonlinear FE tires} \\
\mathbf{M}_s\ddot{\mathbf{e}}_s = \mathbf{Q}_s(\mathbf{e}_t, \mathbf{e}_s, \dot{\mathbf{e}}_t, \dot{\mathbf{e}}_s) \Leftrightarrow \text{RVEs} & \cdots\ \text{Multiscale terrain model} \\
\mathbf{C}(\mathbf{q}_r, \mathbf{e}_t, t) = \mathbf{0} & \cdots\ \text{Joint constraints}
\end{array}\right\} \tag{13}$$

where subscript r, t and s refer, respectively, to rigid bodies, nonlinear FE tire models, and the multiscale soil elements. Mechanical joint constraints and prescribed motion trajectories are imposed on the vehicle components and tires using the kinematic constraint equations,

$\mathbf{C}(\mathbf{q}_r, \mathbf{e}_t, t) = \mathbf{0}$. $\boldsymbol{\alpha}$ is the vector of internal parameters for the composite shell element [25]. For the multiscale terrain model, brick elements integrated in the general multibody dynamics code [6,26] are used as the upper-scale model, while RVE models are developed using an open source DE code, LIGGGHTS (LAMMPS Improved for General Granular and Granular Heat Transfer Simulations) [27]. The upper-scale FE soil model in the multibody dynamics code and the lower-scale RVE models in DE code are then interfaced through the scale-bridging algorithm as will be discussed in Section 3.2.

3.2 Computational Algorithms

3.2.1 Scale-Bridging Algorithm In the upper-scale FE model, the incremental strain tensor at the quadrature point is calculated using Eq. 9 at each time step, and then outputted to define the incremental prescribed strain boundary condition imposed on the RVE model. RVE simulations under the prescribed strain boundary conditions are run in parallel with multiple processors using Message Passing Interface (MPI) as shown in Fig. 2. It is important to notice here that each RVE has no physical interaction with any other RVEs, thus establishing parallel computing scheme for multiple RVEs is more straightforward than the single-scale pure DE model, which requires sophisticated domain decomposition techniques due to strong force coupling between DE subdomains. Having completed the RVE simulation, the homogenized Cauchy stress tensor (Eq. 10) as well as the tangent moduli tensor (Eq. 11) are outputted and passed back to the upper-scale finite element model to calculate the generalized internal forces using Eq. 4 and to define the tangent moduli for the implicit time integrator. It is important to notice here that, for running the large-scale tire-soil interaction simulation with HPC cluster, the scale-bridging algorithm needs to be optimized for the MPI parallel computing since frequent data transfer across multiple compute nodes imposes additional computational burdens in the HPC cluster. For this reason, strain tensor data from the upper-scale FE models are stored in a single file to eliminate multiple file transfer for each RVE and then prescribed strain boundary conditions for all the RVEs are defined directly in the DE script program to eliminate unnecessary file transfer and data read/write processes. Furthermore, REV simulation results at each time step of the upper-scale model are stored in each local storage of each compute node such that it can be used as the initial condition of the RVE in the next time step without unnecessary file transfer across the nodes, as shown in Fig. 2. The homogenized Cauchy stress and tangent moduli tensor data obtained from all the RVEs are also collected in a single file and then passed back to the compute node for the upper-scale model described by Eq. 13.

3.2.2 RVE Initial Packing To run the multiscale simulation, RVEs have to be created using the DE code such that user-defined target confining pressure as well as porosity can be achieved. This process is called RVE initial packing, and an automated initial packing procedure is developed using LIGGGHTS by controlling the RVE volume and inter-particle friction coefficient. First, particles are inserted in an RVE box by specifying the number of particles and particle radius. The particle size distribution can also be specified as needed. Second, the RVE box is incrementally shrunk until the target confining pressure is reached. The friction coefficient between particles is then decreased to reduce porosity of the RVE model. The confining pressure, however, decreases and deviates from the target value due to a decrease in the friction coefficient to lower the porosity. Thus, the RVE box is further shrunk to reach the target confining pressure with the reduced friction coefficient. This procedure is repeated until the target porosity and confining pressure are achieved simultaneously. Finally, the inter-particle friction coefficient is set back to the actual value to create the initially-packed RVE model.

3.2.3 Moving Soil Patch Technique In the off-road mobility simulation, a wider range of terrain needs to be considered as the vehicle's traveling distance increases and it results in a large-scale computational terrain model needed in the analysis. For this reason, the moving soil patch technique introduced for FE terrain model [6] is extended for the multiscale soil model to reduce computational intensity as well as the soil model dimensionality. In this technique, a soil patch is defined in the vicinity of a traveling tire such that soil elements behind the tire are removed as the tire moves forward, while new elements are being added ahead of the tire. This allows for maintaining the same terrain model size regardless of the traveling distance, thereby resulting in computational time proportional to the traveling distance, as demonstrated in the literature [6]. For the multiscale model, multiscale elements with initially packed RVEs are added sequentially. Furthermore, since the element deformation data as well as the particle data in RVEs are saved, the eliminated elements behind the tire can be recovered whenever the soil patch of the other tire enter into that region. In other words, deformable terrain behavior due to multiple tire passage can be considered without loss of generality.

4. MULTISCALE SOIL SIMULATION AND VALIDATION

In what follows, several numerical examples are presented in order to demonstrate capabilities of the hierarchical FE-DE multiscale soil model.

4.1 Triaxial Compression Test Simulation

In order to validate the hierarchical FE-DE multiscale soil model implemented in the multibody dynamic computer algorithm, a triaxial compression soil test model is developed and then results are compared with the test data as well as the pure DE simulation results. The soil specimen is consolidated by applying a uniform confining pressure of 25 kPa and then the deviatoric stress is applied vertically to obtain the stress and strain relationship. The volume, height, and the crosssection diameter of the initial specimen are 564.86 cm^3, 142.27 mm, and 71.10 mm, respectively. The water content is 11.20% and the dry density of the specimen is 1.933 g/cm^3 [6]. The DE model parameters are calibrated using a pure DE model with LIGGGTHS and the following parameters are used in this study: $E = 1.5\times10^9$ Pa , $\nu = 0.293$, $\mu = 0.452$, $\beta = 2.25$, and $\eta = 0.99$. Numerical results obtained using a different number of particles are compared with the test data in Fig 3. For simplicity, spherical particles are assumed with constant particle radius of 0.87 mm. It is observed from this figure that an increase in the number of particles leads to a convergent solution and use of 160,000 particles results in good agreement with the test result. The stress-strain curve exhibits noticeable post-failure softening behavior due to the low confining pressure applied.

The hierarchical FE-DE multiscale model for this triaxial compression test scenario is developed with the DE parameters used for the pure DE model. The stress-strain curves obtained using 1 and 8 elements with 1,000 and 2,000 particles per RVE are presented in Fig. 4 and they are compared with the pure DE and test results. It is observed from this figure that use of 1,000 and 2,000 particles per RVE leads to the solution that is in agreement with the original pure DE model as well as the test data. Furthermore, use of single element with 8 quadrature points (i.e., 8 RVEs) is good enough to obtain accurate solution in this triaxial test condition and the result is in good agreement with that of the 8 element model with 64 RVEs. The computation time of the single element model with 8 RVEs with 2,000 particles is 951 sec using 8 processors, while that of the pure DE model with 160,000 particles is 42,360 sec using 32 processors and 9,720 sec using 512 processors. Since the DE simulation is performed only at the quadrature points using RVEs, the model dimensionality is much smaller than the pure DE model, resulting in substantial reduction in computational time while maintaining the same accuracy. It is also important to notice here that, for the multiscale model, one processor is used to run each RVE simulation due to small number of particles (1,000 or 2,000) used in the RVE, while MPI parallelization is used to run multiple RVE models concurrently.

While the 8-RVE model is good enough to obtain the result that agrees well with the pure DE model, the parallel computing scalability analysis is performed for the multiscale model with different number of elements (1, 8 and 64). 2000 particles are assumed in these models and the results are shown in Fig. 5. Since there are 8 quadrature points per element, these models have 8, 64, and 512 RVEs, respectively. It is observed from Fig. 5 that similar scalability characteristics are achieved regardless of the number of elements. The RVE models in the multiscale model are independent and there is no force coupling among them, thus good parallel computing scalability can be achieved regardless of the number of RVEs considered in the model. Maintaining good parallel computing scalability is critically important in this study since off-road mobility simulation requires a large number of multiscale elements and one can then gain substantial benefit from the high-performance computing capability of the multiscale tire-soil interaction simulation. Furthermore, computational times of the three multiscale models obtained using their maximum of number of processors (i.e., the number of processors = the number of RVEs) are in the similar range. A slight increase in the computational time for larger number of elements can be attributed to increasing computational cost for the solution process of the upper-scale model (i.e., FE model) as well as increasing communication time between the upper and lower-scale models. Nevertheless, the computational time is still substantially lower than that of the pure DE model, and the higher computational efficiency of the hierarchical multiscale soil model, as compared to the pure DE model, is clearly evident from this result.

4.2 Shear Band Failure Simulation

In the next example, the shear band failure of biaxial compression test specimen is discussed. This simulation is used to demonstrate soil modeling capabilities for predicting complex strain localization behavior of geomaterials [21,22]. As shown in Fig. 6, the length, width, and thickness of the biaxial test specimen are 80 mm, 40 mm, and 10 mm, respectively. The confining pressure is assumed to be 200 kPa. The bottom left corner of the specimen is fixed to the ground, while the other nodes on the bottom surface are free to move in the horizontal axis [22]. Thus, compressing the top surface causes a diagonal failure band, called shear band failure. The DE parameters for RVEs are assumed to be same as the previous triaxial test example and 2000 particles per RVE are considered. The deformed shape and the compressive normal strain distribution ε_{33} are shown in Fig. 7 for different number of elements at the axial strain of 8 %. The localized shear band failure is clearly observed in this figure and an increase in the number elements results in the band width narrower. To further discuss the element convergence, the deviatoric stress is presented as a function of the axial compressive strain in Fig. 8. It is observed from this figure that the shear band failure is initiated around the axial strain of 5 % and use of 512 elements ($16\times1\times32$) leads to the convergent solution. This example demonstrates the potential of the hierarchical multiscale soil model in predicting the localized failure of soil under a rolling tire with traction, as experimentally observed by particle image velocimetry (PIV) approach [28].

5. MULTISCALE TIRE-SOIL INTERACTION SIMULATION

5.1 Test Condition and Simulation Model

To validate the multiscale tire-soil interaction simulation capability developed in this study, the off-road mobility soil bin test results are used for comparison [6]. A commercial off-road tire of 235/75R15 used in the test is modeled with the nonlinear shear deformable composite shell element based on the absolute nodal coordinate formulation and details on the modeling procedure and validation of the tire model are found in the literature [25]. The traveling speed of the tire is 1 m/s and the tire attached to the moving carriage is free to rotate about its spin axis without traction. Two different wheel loads of 6 and 8 kN are considered, for which three tire inflation pressures of 180, 230, and 280 kPa are tested. The steering angle is set to zero. The tire forces are measured by the 3-axis tire force transducer embedded in the rim, while the soil sinkage is measured in the middle of the rut by a depth sensor. Soil sample data was collected from the soil bin in different test cases. The mean soil density is 1,556 kg/m^3, the mean water content is 8.21%, and the mean void ratio, defined as a ratio of the volume of void space to the volume of solids, is 0.893. Those values are used to determine parameters for the lower-scale DE RVE models. The other DE parameters are assumed to be same as those of the triaxial compression test model since the same soil is used in both tests. The running test is repeated twice for each test scenario. The soil is not compacted by a roller in each test condition.

In the simulation model, the moving soil patch length, width and height are, respectively, 1.0 m, 0.48 m and 0.4 m. The soil patch width is selected such that the boundary effect is negligible. The soil patch is updated and shifted forward at every traveled distance of 0.2 m of the tire. This results in the tire-soil interaction occurring around the center of the patch and the boundary effect can be neglected. The number of elements for the soil patch is 2,400, while the total number of RVEs is 19,200. Each RVE has 2,000 particles with the particle radius of 0.87 mm as in the triaxial soil test model. The void ratio of the RVE is set to be the same as the measured data and the initial confining pressure is assumed to be zero since the soil is not compacted after loosening the soil in each test scenario.

5.2 Numerical Results and Experimental Validation

The deformed shapes of the rolling tire on the multiscale soil with the moving soil patch technique are shown in Fig. 9 along with the von Mises stress distribution under the vertical load of 6 kN and the tire inflation pressure of 230 kPa. The deformed shapes of RVEs at different location in the soil are also shown in Fig. 9. Compressive deformation is dominant in the RVE at positon (a) since the soil is compacted after the tire rolls over this portion, while noticeable compressive and shear deformation is exhibited in the RVE at position (b) under the rolling tire. The RVE ahead of the tire at position (c) remains initially packed, while shear deformation is observed for the RVE at position (d) around the edge of the rut. As such, use of the hierarchical multiscale model allows for facilitating cross-scale understanding of the soil behavior resulting from the interaction with the rolling tire. The tire forces obtained by the test and the simulation are compared in Figs. 10 (a) and (b) for the wheel load of 6 and 8 kN, respectively. The coefficient of friction is assumed to be 0.25. Since the vertical wheel load is regulated, the vertical force Fz must be in good agreement. The lateral force Fy is zero due to zero steering angle. The longitudinal force Fx represents the rolling resistance force of the tire. The larger wheel load leads to larger longitudinal forces. The simulation and test results are in good agreement in magnitude. To further discuss the effect of the wheel loads and tire inflation pressure on the mobility performance, the soil sinkage is compared with the test data in Fig. 11, while the longitudinal tire force as well as the rolling resistance coefficient are shown in Figs. 12

and 13 under various wheel load and tire inflation pressure conditions. The test results are shown with error bars. It is observed from Fig. 11 that an increase in the wheel load causes an increase in the soil sinkage as expected and higher inflation pressure results in larger sinkage due to higher contact pressure developed in the contact patch. Despite the variability of the sinkage test data due to measurement by hand, the results agree reasonably well. Furthermore, it is observed from Fig. 12 that the longitudinal tire force increases as the wheel load and tire inflation pressure increase. That is, large sinkage resulting from higher tire inflation pressure causes larger resistance force exerted on the tire. This trend is well captured in the simulation model and the tire forces are in good agreement with the test data for different wheel loads and inflation pressures. It is also observed from Fig. 13 that the rolling resistance coefficient (Fx/Fz) increases as the tire inflation pressure increases, while it remains almost constant and less sensitive to the wheel loads in both simulation and test results. The parallel computing scalability is showed in Fig. 14 for this tire-soil interaction model, where computational time per iteration is effectively decreased as the number of processors increases, as in the triaxial compression test example. That is, the MPI parallelization for the lower-scale RVEs as well as the OpenMP parallelization for the upper-scale FE-based flexible multibody model models work properly. The CPU time for the tire traveling a distance of 1.0 m is approximately 27 hours with HPC cluster, Intel Broadwell, 2.4 GHz, while use of the pure DE model with the same particle size (i.e., 0.87 mm) requires excessively large number of particles and computational time.

While the tire traction test data is unavailable, the tire force characteristics are calculated using the flexible tire rolling over the multiscale terrain model as shown in Fig. 15 under three different tire inflation pressures. The slip ratio is defined by $s=(R\omega-V)/R\omega$, where R is the effective rolling radius, ω is the rim angular velocity, and V is the forward velocity which is set to 1.0 m/s. In the small slip ratio range, the longitudinal force is negative since the resistance force from the soil deformation is higher than the driving force exerted on the tire. As the slip ratio increases, on the other hand, the longitudinal force becomes positive around the slip ratio of 18 %, i.e., the driving force exceeds the resistance force. The rate of increase changes around the slip ratio of 40 % and the longitudinal force increase gradually as the slip increases. Furthermore, it is observed from this result that higher inflation pressure results in lower longitudinal forces due to larger resistance force exerted by soil resulting from higher soil sinkage, as observed in test data [30]. This fundamental traction characteristics are captured with the proposed multiscale tire-soil interaction simulation model.

6. SUMMARY AND CONCLUSIONS

While a wide variety of computational tire-soil interaction models have been proposed using FE approaches, use of phenomenological constitutive assumptions in FE soil models makes the modeling of complex granular soil behavior very difficult due to highly nonlinear anisotropy of soil strength and strain localization exhibited in the tire-soil interaction. DE models, therefore, has gained acceptance in predicting complex granular soil behavior. DE simulation is, however, computational very intensive, especially when considering a wide range of deformable terrain for off-road mobility simulation. To address the limitations of existing single-scale FE and DE terrain models, a hierarchical FE-DE multiscale tire-soil interaction simulation capability, which can be fully integrated in the general multibody dynamics computer algorithm, was developed in this study for high-fidelity off-road mobility simulation. The terrain deformation is modeled by FE meshes, while the stress response of complex granular material within the element is predicted by physical RVE models using DE approach. For this, incremental true strains at element quadrature points are converted to prescribed strain boundary conditions imposed on corresponding RVE models and the homogenized Cauchy stress tensor is then given back to the upper-scale FE model for defining the generalized internal forces. Each lower-scale RVE model is independent and there are no physical interactions with the other RVEs. Thus, multiple DE simulations were parallelized with MPI, while the share-memory parallel computing is used for solving the multibody dynamics equations with the upper-scale soil models with OpenMP. It was shown that high parallel computing scalability was maintained regardless of the number of multiscale elements considered. Using the triaxial compression test model, it was demonstrated that computational cost can be substantially lowered by the multiscale soil model as compared to the corresponding pure DE model while maintaining the same accuracy. This was attributed to the smaller number of DE particles that can be used in the model and high parallel computing scalability achieved. The multiscale tire-soil interaction model was developed using the multibody-dynamics based multiscale computational framework developed in this study and the moving soil patch technique was generalized for the multiscale terrain model to maintain the terrain model dimensionality the same regardless of the traveling distance considered. The simulation results were validated against the soil bin mobility test data for the soil sinkage, longitudinal force, and the rolling resistance coefficient under various wheel load and tire inflation pressure conditions, thereby demonstrating the potential of the proposed approach to resolve challenging vehicle-terrain interaction problems. This approach is currently further extended for full vehicle simulations with improved computational load balancing for lower scale models [31].

ACKNOWLEDGEMENTS

This research is supported by the Automotive Research Center (ARC) in accordance with Cooperative Agreement W56HZV-04-2-0001 U.S. Army Tank Automotive Research, Development and Engineering Center (TARDEC).

DISCLAIMER

Reference herein to any specific commercial company, product, process, or service by trade name, trademark, manufacturer, or otherwise, does not necessarily constitute or imply its endorsement, recommendation, or favoring by the United States Government or the Department of the Army (DoA). The opinions of the authors expressed herein do not necessarily state or reflect those of the United States Government or the DoA, and shall not be used for advertising or product endorsement purposes.

REFERENCES

[1] McCullough, M., Jayakumar, P., Dasch, J., and Gorsich, D., 2017, “The Next Generation NATO Reference Mobility Model Development”, *Journal of Terramechanics*, vol. 73, pp.49-60.

[2] Helwany, S., 2007, *Applied Soil Mechanics with ABAQUS Applications*, John Wiley and Sons, New York.

[3] Shoop S. A., 2001, "Finite Element Modeling of Tire-Terrain Interaction", *Cold Regions Research and Engineering Laboratory*, ERDC/CRREL TR-01-16, pp. 1-59.

[4] Xia, K., 2011, "Finite Element Modeling of Tire/Terrain Interaction: Application to Predicting Soil Compaction and Tire Mobility", *Journal of Terramechanics*, vol. 48, pp.113-123.

[5] Li, H. and Schindler, C., 2012, "Three-Dimensional Finite Element and Analytical Modelling of Tyre-Soil Interaction", *IMechE Journal of Multi-Body Dynamics*, vol. 227, pp. 42-46.

[6] Yamashita, H., Jayakumar, P., Alsaleh, M. and Sugiyama, H., 2018, "Physics-Based Deformable Tire-Soil Interaction Model for Off-Road Mobility Simulation and Experimental Validation", *ASME Journal of Computational and Nonlinear Dynamics*, vol. 13, pp.021002-1-15.

[7] Cundall, P. A. and Strack, O. D. L., 1979, "Discrete Numerical Model for Granular Assemblies", *Geotechnique*, vol. 29, pp. 47-65.

[8] O'Sullivan, C., 2011, *Particulate Discrete Element Modelling: A Geomechanics Perspective*, Routledge.

[9] Smith, W. and Peng, H., 2013, "Modeling of wheel–soil interaction over rough terrain using the discrete element method", *Journal of Terramechanics*, vol. 50, pp. 277–287.

[10] Negrut, D., Serban, R., Mazhar, H., Heyn, T., 2014, "Parallel Computing in Multibody System Dynamics: Why, When and How”, *ASME Journal of Computational and Nonlinear Dynamics*, vol. 9, 041007.

[11] Wasfy, M. T., Jayakumar, P., Mechergui, D., and Sanikommu, S., 2016, "Prediction of Vehicle Mobility on Large-Scale Soft-Soil Terrain Maps Using Physics-Based Simulation", *Proceedings of 2016 NDIA Ground Vehicle Systems Engineering and Technology Symposium* (GVSETS), Novi, MI.

[12] Recuero, A., Serban, R., Peterson, B., Sugiyama, H., Jayakumar, P. and Negrut, D., 2017, "High-Fidelity Approach for Vehicle Mobility Simulation: Nonlinear Finite Element Tires Operating on Granular Material", *Journal of Terramechanics*, vol. 72, pp. 39-54.

[13] Tasora, A., Serban, R., Mazhar, H., Pazouki, A., Melanz, D., Fleischmann, J., Taylor, M., Sugiyama, H. and Negrut, D., 2016, "Chrono: An Open Source Multi-physics Dynamics Engine", *High Performance Computing in Science and Engineering - Lecture Notes in Computer Science* (Eds., Kozubek, T., Blaheta, R., Šístek, J., Rozložník, M. and Cermák, M.), Springer, pp. 19-49.

[14] Serban, R., Olsen, N., Negrut, D., Recuero, A., Jayakumar, P. and 2017, "A Co-Simulation Framework for High-Performance, High-Fidelity Simulation of Ground Vehicle-Terrain Interaction", *NATO AVT-265,* pp. 1-22.

[15] Pazouki, P., Kwarta, M., Williams, K., Likos, W., Serban, R., Jayakumar, P. and Negrut, D., 2017, "Compliant Contact versus Rigid Contact: A Comparison in the Context of Granular Dynamics", *Physical Review E,* vol. 96, pp. 042905.

[16] Nakashima, H. and Oida, A, 2004, "Algorithm and Implementation of Soil–Tire Contact Analysis Code Based on Dynamic FE–DE Method", *Journal of Terramechanics,* vol. 41, pp. 127-137.
[17] Rojec, J. and Onate, E., 2007, “Multiscale Analysis Using a Coupled Discrete/Finite Element Model”, *Interaction and Multiscale Mechanics*, vol.1, pp.1-31
[18] Regueiro, R.A. and Yan, B., 2011, “Concurrent Multiscale Computational Modeling for Dense Dry Granular Materials Interfacing Deformable Solid Bodies”, *Geomechanics and Geoengineering*, pp.251-273.
[19] Meier, H. A., Steinmann, P., and Kuhl, E., 2008, "Towards Multiscale Computation of Confined Granular Media - Contact Forces, Stresses and Tangent Operators", *Technische Mechanik*, vol. 28, pp.32-42.
[20] Andrade, J. E., Avila, C. F., Hall, S. A., Lenoir, N. and Viggiani, G., 2011, "Multiscale Modeling and Characterization of Granular Matter: From Grain Kinematics to Continuum Mechanics", *Journal of the Mechanics and Physics of Solids*, vol. 59, pp.237-250.
[21] Guo, N. and Zhao, J., 2014, "A Coupled FEM/DEM Approach for Hierarchical Multiscale Modeling of Granular Media", *International Journal for Numerical Methods in Engineering*, vol.99, pp.789-818.
[22] Liu, Y., Sun, W. C., Yuan, Z. and Fish, J., 2015, "A Nonlocal Multiscale Discrete-Continuum Model for Predicting Mechanical Behavior of Granular Materials", *International Journal for Numerical Methods in Engineering*, vol.106, pp.129-160.
[23] de Souza Neto, E. A., Peric, D. and Owen, D. R. J., 2008, *Computational Methods for Plasticity: Theory and Applications*, Wiley
[24] Ai, J., Chen, J-F, Rotter, J.M., Ooi, J.Y., 2011, "Assessment of Rolling Resistance Models in Discrete Element Simulations", *Powder Technology*, vol. 206, pp. 269-282.s
[25] Yamashita, H., Valkeapää, A., Jayakumar, P., Sugiyama, H. and 2015, "Continuum Mechanics Based Bilinear Shear Deformable Shell Element Using Absolute Nodal Coordinate Formulation", *ASME Journal of Computational and Nonlinear Dynamics*, vol. 10, 051012-1-9.
[26] Sugiyama, H. and Yamashita, H., 2011, "Spatial Joint Constraints for the Absolute Nodal Coordinate Formulation Using the Non-Generalized Intermediate Coordinates", *Multibody System Dynamics*, vol. 26, pp. 15-36.
[27] Kloss, C., Goniva, C., Hager, A., Amberger, S. and Pirker, S., 2012, "Models, algorithms and validation for opensource DEM and CFD-DEM", *Progress in Computational Fluid Dynamics, An International Journal*, vol. 12, pp.140-152
[28] Senatore, C., Wulfmeier, M., Vlahinić, I., Andrade, J. and Iagnemma, K., 2013, "Design and Implementation of a Particle Image Velocimetry Method for Analysis of Running Gear–Soil Interaction", *Journal of Terramechanics,* vol. 50, pp. 311-326.
[29] Yamashita, H., Jayakumar, P. and Sugiyama, H., 2016, "Physics-Based Flexible Tire Model Integrated with LuGre Tire Friction for Transient Braking and Cornering Analysis", *ASME Journal of Computational and Nonlinear Dynamics*, vol. 11, pp.031017-1-17.
[30] Wong, J. Y. 2008, *Theory of Ground Vehicle. 4th ed.* Hoboken, NJ: John Wiley & Sons.
[31] Knap, J., Spear, C., Leiter, K., Becker, R. and Powell, D., 2016, “A Computational Framework for Scale-Bridging in Multi-Scale Simulations”, *International Journal for Numerical Methods in Engineering*, vol. 108, pp. 1649-1666.

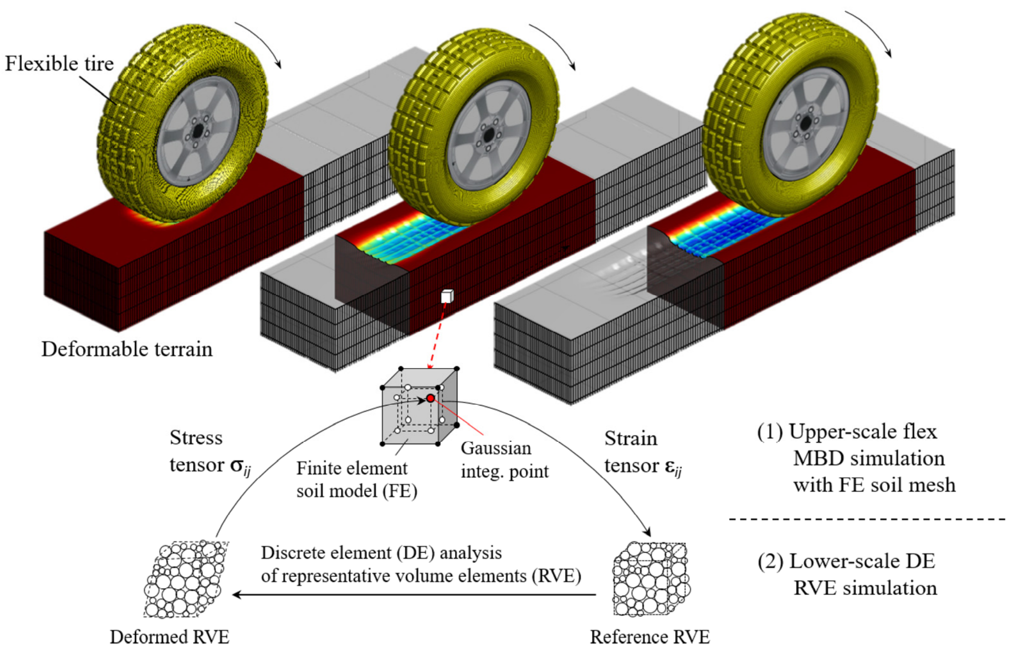

Figure 1 Hierarchical multiscale tire-soil interaction simulation model

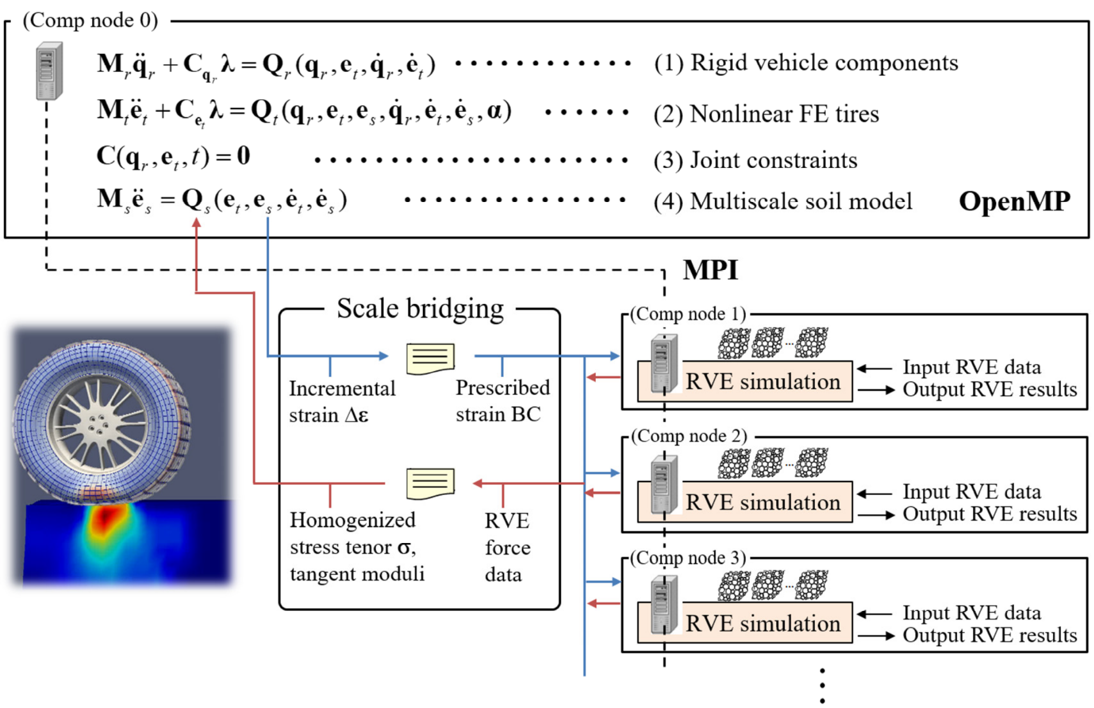

Figure 2 Parallelized scale-bridging algorithm for hierarchical multiscale tire-soil interaction simulation capability

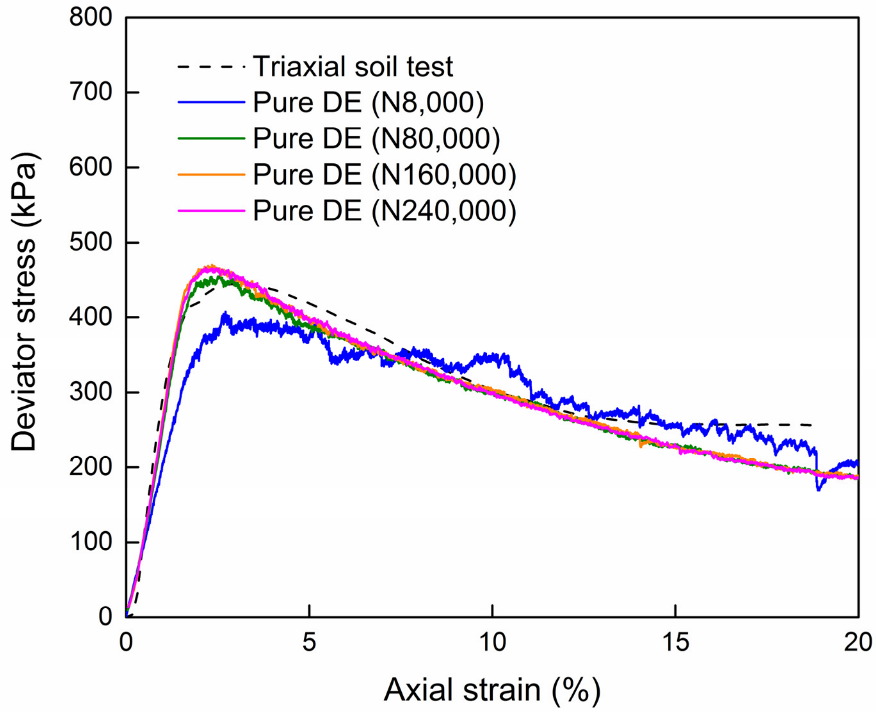

Figure 3 Stress-strain curve using pure DE soil model

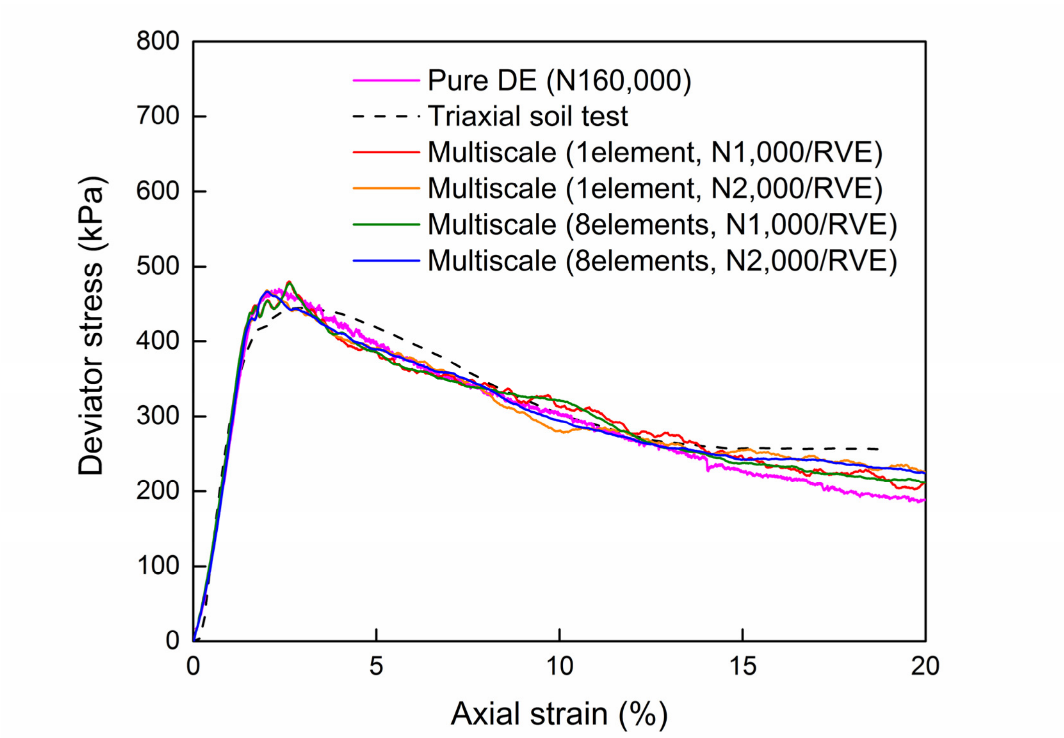

Figure 4 Stress-strain curve of multiscale soil model

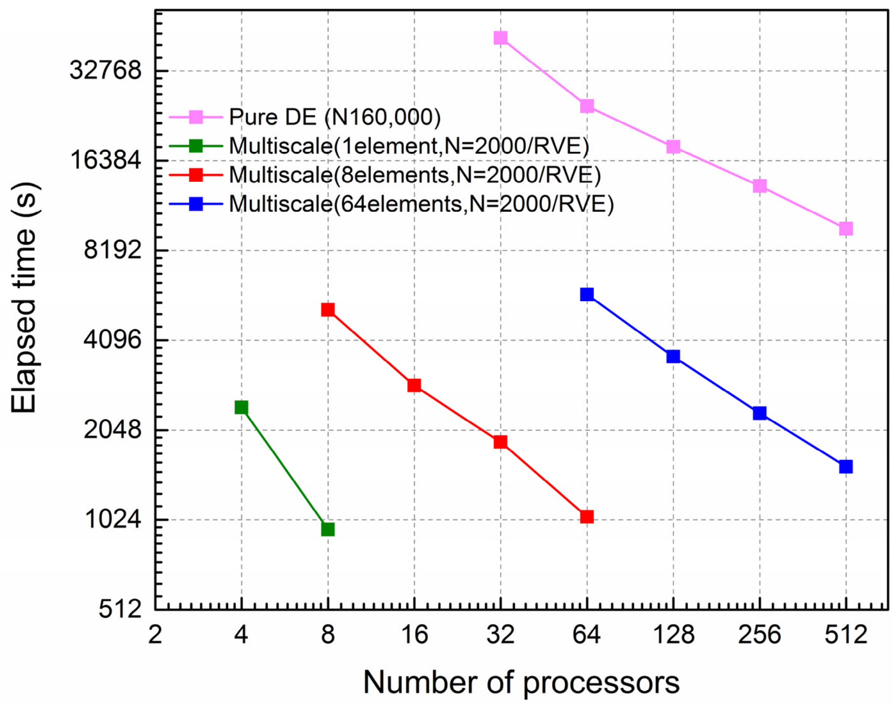

Figure 5 Parallel computing scalability of multiscale and pure DE models

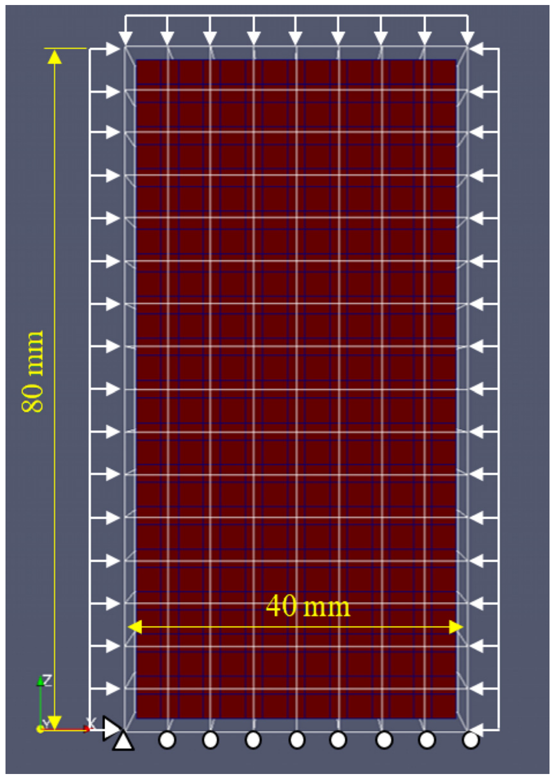

Figure 6 Biaxial compression test model

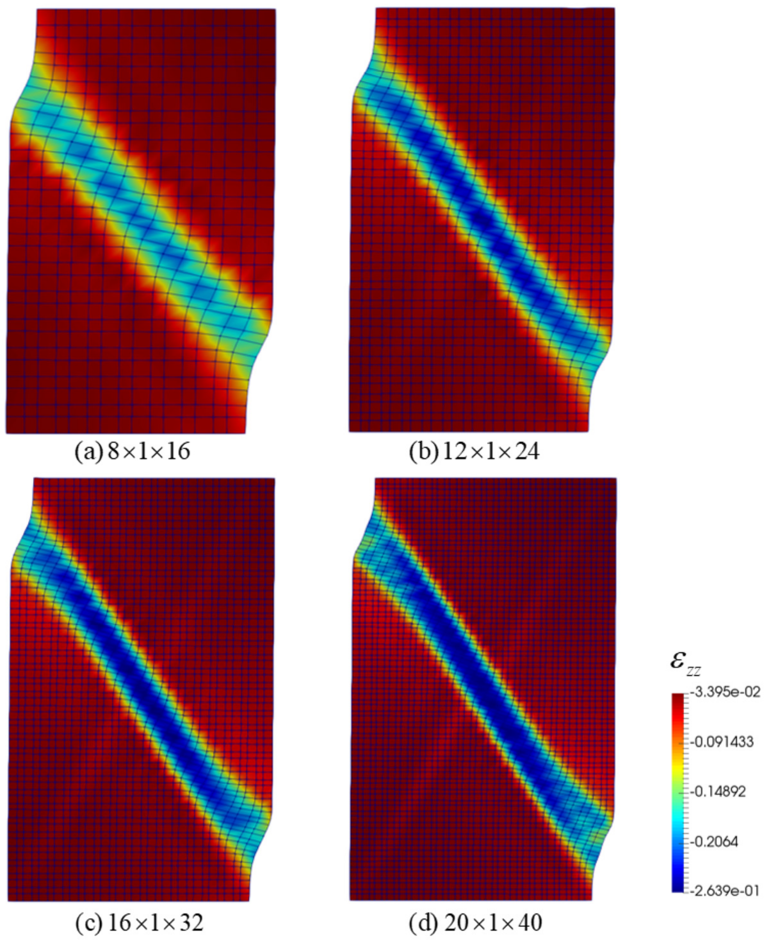

Figure 7 Shear banding failure at 8% axial strain predicted by multiscale soil model

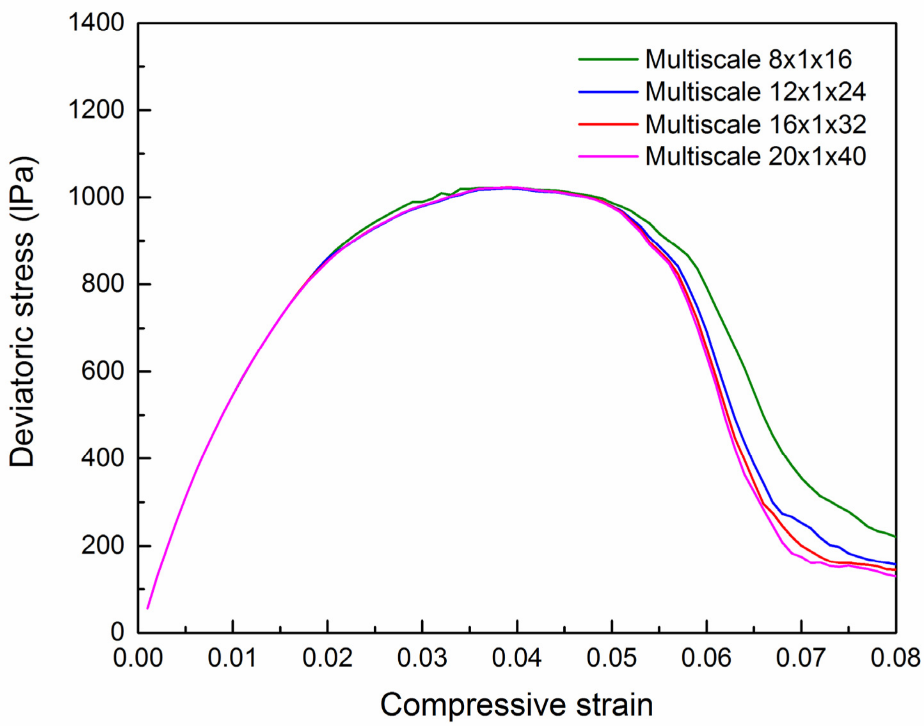

Figure 8 Effect of number of multiscale elements

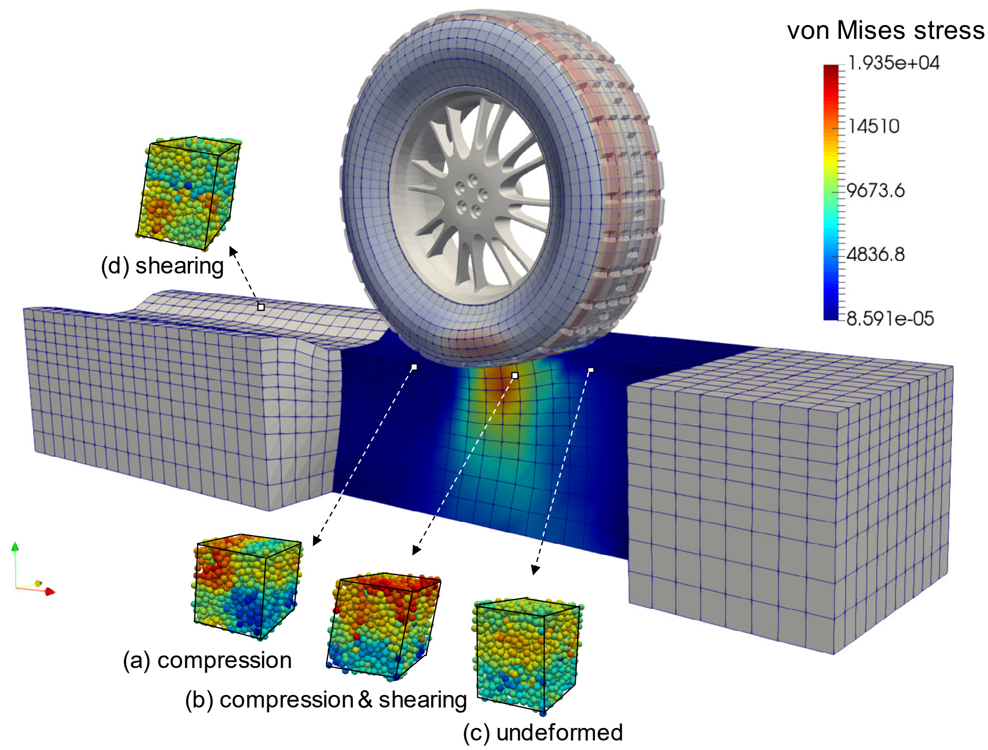

Figure 9 Multiscale tire-soil interaction simulation using moving soil patch approach

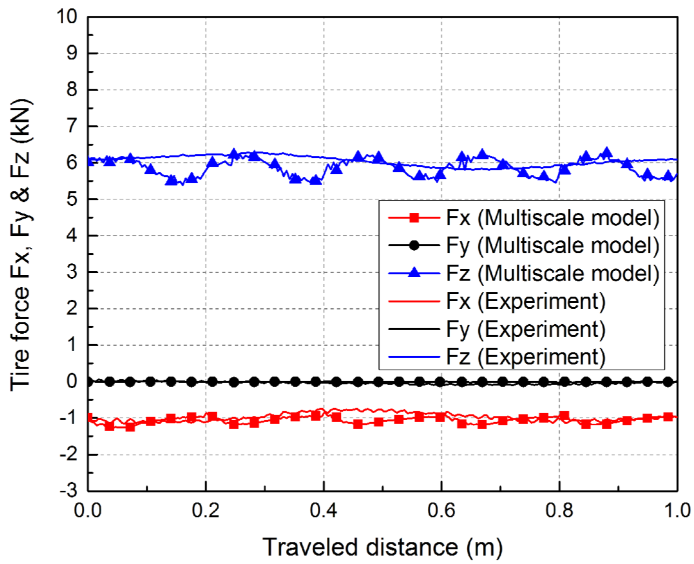

(a) Wheel load: 6kN

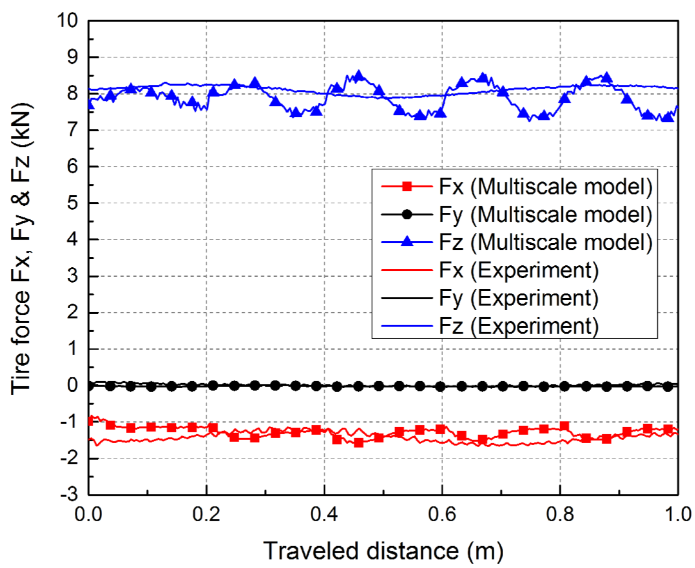

(b) Wheel load: 8kN

Figure 10 Comparison of tire forces for 6kN and 8kN wheel load with 230 kPa inflation pressure

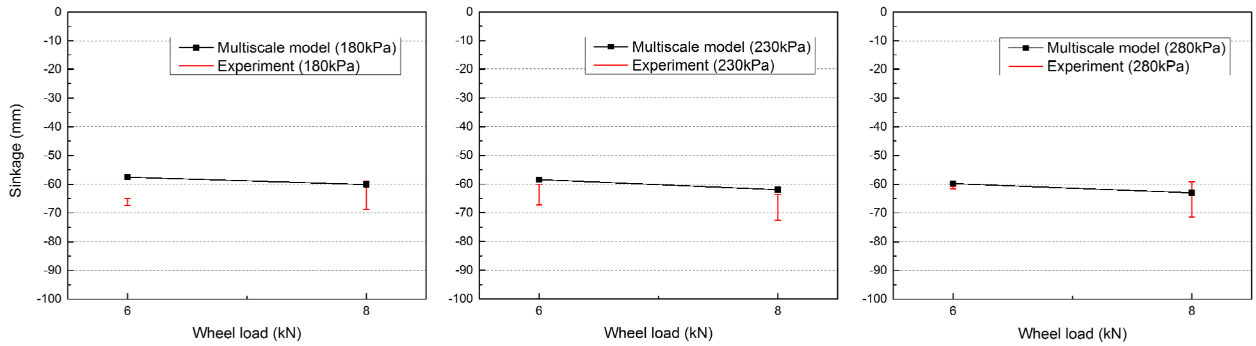

Figure 11 Soil sinkage for different wheel loads and tire inflation pressure

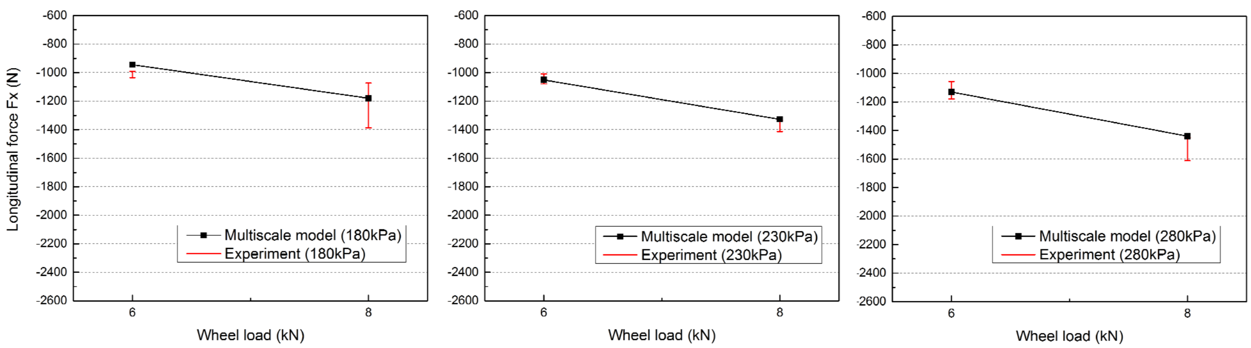

Figure 12 Longitudinal tire force (Fx) for different wheel loads and tire inflation pressure

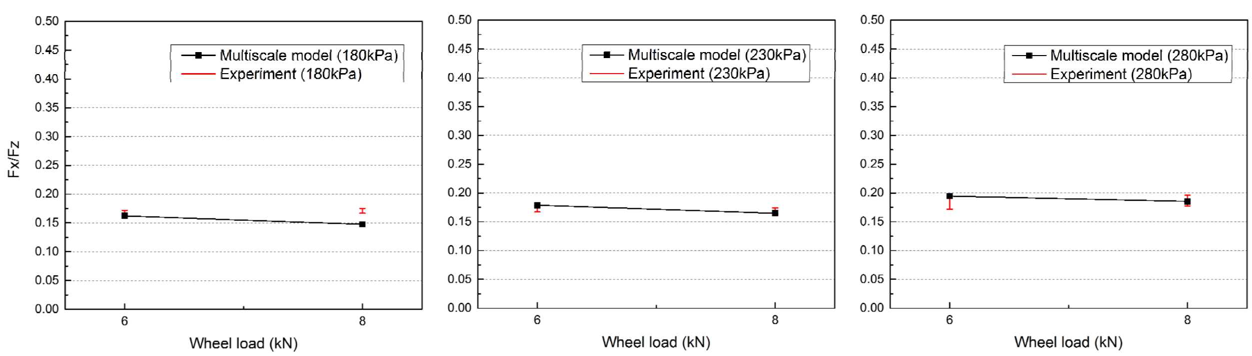

Figure 13 Rolling resistance (Fx/Fz) for different wheel loads and tire inflation pressure

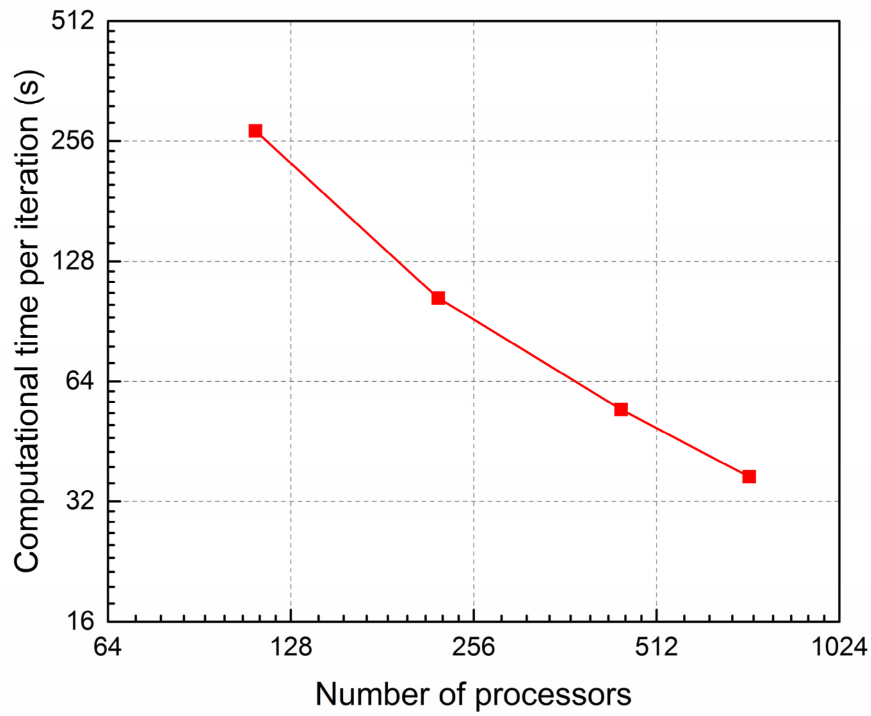

Figure 14 Parallel computing scalability of multiscale tire-soil interaction model

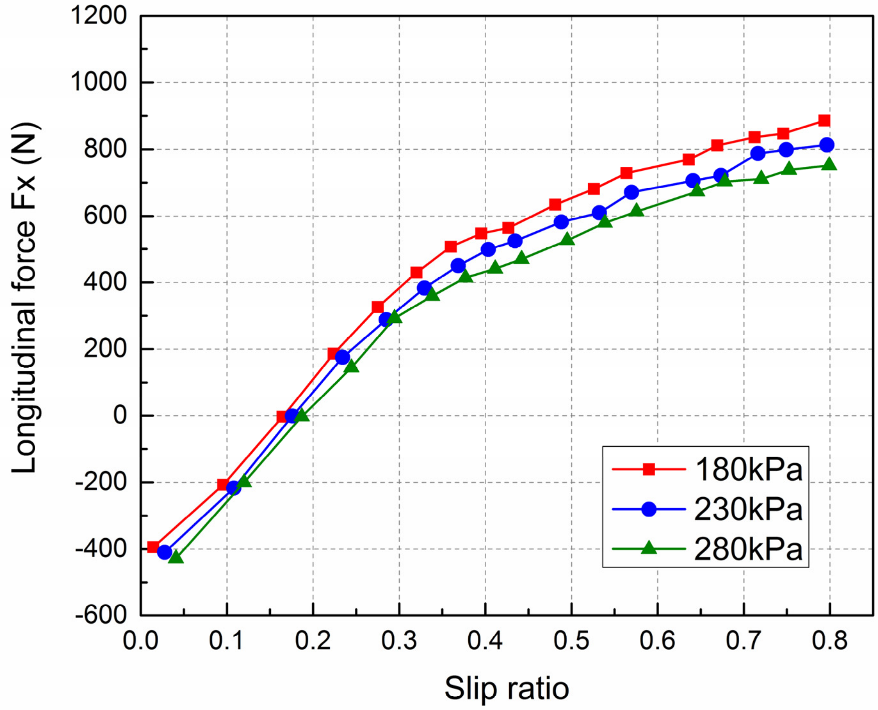

Figure 15 Longitudinal tire force characteristics on deformable soil